Biosensors and Bioelectronics 26 (2010) 991–995

Contents lists available at ScienceDirect

Biosensors and Bioelectronics

journal homepage: www.elsevier.com/locate/bios

A novel nitromethane biosensor based on biocompatible conductive redox graphene-chitosan/hemoglobin/graphene/room temperature ionic liquid matrix

Lu Wang, Xiuhua Zhang, Huayu Xiong, Shengfu Wang*

Ministry-of-Education Key Laboratory for the Synthesis and Application of Organic Functional Molecules, College of Chemistry and Chemical Engineering, Hubei University, 11 Xueyuan Road, Wuhan 430062, China

ARTICLE INFO

Article history:
Received 10 May 2010
Received in revised form 21 July 2010
Accepted 12 August 2010
Available online 19 August 2010

Keywords:
Hemoglobin
Graphene
Room temperature ionic liquid
Nitromethane
Electrocatalysis

ABSTRACT

A novel amperometric biosensor for nitromethane (CH_3NO_2) based on immobilization of graphene (GR), chitosan (CS), hemoglobin (Hb) and room temperature ionic liquid (IL) on a glassy carbon electrode (GCE) was developed for the first time. The surface morphologies of a set of representative membranes were characterized by means of scanning electron microscopy (SEM). The electrochemical performance of the biosensor was evaluated by cyclic voltammetry (CV) and chronoamperometry. A pair of stable and well-defined redox peaks of Hb with a formal potential of −0.240 V was observed at the GR-CS/Hb/GR/IL/GCE. The effects of phosphate buffer pH, scan rate, and temperature on the biosensor were investigated to provide optimum analytical performance. Moreover, several electrochemical parameters, e.g., the heterogeneous electron transfer rate constant (k_s), were calculated in detail. The presence of both GR and IL not only dramatically facilitated the electron transfer of Hb, but also greatly enhanced electrocatalytic activity towards CH_3NO_2. The apparent Michaelis–Menten constant was down to 0.16 μM, indicating that the biosensor possessed high affinity to CH_3NO_2. Besides this, the proposed biosensor exhibited fast amperometric response (<5 s), low detection limit (6.0×10^{-10} M), and excellent long-time storage stability for the determination of CH_3NO_2.

1. Introduction

Organic nitro compounds have attracted a great deal of interest over the past decades because of the widespread use of these compounds as explosive materials (Fainberg, 1992), fuels (Sabourin et al., 2009), special solvents (Subirats et al., 2005), and even as chemical coatings (Wang et al., 1998). Nitromethane (CH_3NO_2), the simplest of the aliphatic nitro compounds, is one of the most common pollutants with relatively high vapor pressure (Jean and Mekki, 2004; Singh, 2007). The chronic exposure to nitromethane leads to many critical effects on human health such as thyroid toxicity, blood dyscrasias and peripheral neuropathy (Page et al., 2001). Hence, extensive efforts have been devoted to the detection of CH_3NO_2 including colorimetry (Jones and Riddick, 1956), solid-phase microextraction (SPME)-gas chromatography (GC)–high resolution mass spectrometry (HRMS) (SPME-GC–HRMS) (Alwis et al., 2008), fluorimetry (Meaney and McGuffin, 2008). However, a majority of these methods suffered from limitations. For instance, fluorescence spectrometry demands large samples in despite of the high sensitivity. Nowadays, electrochemical method appears much more elegant to be used to detect CH_3NO_2 mainly due to specificity, fast, and ease of monitoring (Singh, 2007). However, to the best of our knowledge, very little work has been performed on the determination of CH_3NO_2 by the direct electrochemical measurement with the enzyme electrode.

It is well known that enzyme-based method shows fast speed, high sensitivity and good selectivity. So, the electrochemical studies of enzyme and proteins are of considerable importance in biosensors and biocatalysts. To date, a variety of materials have been employed as modifiers to realize direct electron transfer of metalloproteins (e.g., hemoglobin (Hb)), such as surfactant (Liu et al., 2007), lipid (Tang et al., 2003), hydrogel polymer (Liu et al., 2004) and nanomaterials (Xu et al., 2009). Graphene (GR) as a "rising star" carbon nanomaterial has become a hot topic in myriad of research areas during recent years (Sabourin et al., 2009; Chen et al., 2009). It was reported that GR exhibits high surface area and excellent electrical conductivity (Stankovich et al., 2006). From this it is clear that the increase of effective surface area is helping for introducing a larger number of active sites. The high conductivity can facilitate the electron transfer of electroactive species. With those advantages, a number of electrochemical sensors and biosensors based on GR were successfully developed for analytical purposes (Wang et al., 2009; Shan et al., 2009; Kang et al., 2009). More recently, increasing attention has been paid to the modified electrodes with GR and room temperature ionic liquid (IL) in hopes of synergizing their exceptional properties (Shan et al., 2010; Liu et al., 2010).

* Corresponding author. Tel.: +86 27 50865309; fax: +86 27 88663043.
E-mail address: wangsf6@yahoo.com.cn (S. Wang).

0956-5663/$ – see front matter © 2010 Elsevier B.V. All rights reserved.
doi:10.1016/j.bios.2010.08.027

IL is an ionic compound composed of bulky asymmetric cations and small anions, which preserves liquid state over a wide temperature range (Moulthrop et al., 2005). It possesses many fascinating properties like low toxicity, negligible vapor pressure, wide potential window, high thermal stability, good conductivity and electrochemical stability (Quinn et al., 2002). Therefore, IL suggests a great potential application in various areas. In the field of electroanalysis, the applications of IL generally focus on two aspects. One is that IL is served as an alternative solvents or supporting electrolyte (Wang et al., 2005). For example, our groups had explored the direct electrochemical and electrocatalysis of heme proteins immobilized by agarose hydrogel films in IL (Wang et al., 2005). On the other hand, IL is used as modified material in application of biosensors and biocatalysis (Chen et al., 2007). This has gained more and more attentions in recent years. Chitosan (CS) is an abundant natural-bioploymer with unique structure. It has been universally used to disperse nanomaterials and immobilize enzymes owing to its good water permeability, excellent film forming ability, biocompatibility, nontoxicity, and high mechanical strength (Zhang et al., 2004).

Herein, a novel nitromethane biosensor with sandwich structure (GR-CS/Hb/GR/IL) was fabricated by integrating the advantageous features of GR, IL, and CS. The electrochemical properties of this biosensor were investigated including the direct electron transfer of Hb and electrochemical determination of CH_3NO_2. Besides, the special sandwich structure played a crucial role in retaining the bioactivity of Hb and avoiding the leakage of the immobilized protein.

2. Experimental

2.1. Reagents and apparatus

GR (kindly provided by Professor Xianbao Wang from Faculty of Materials Science and Engineering, Hubei University, China) were used as received. The room temperature ionic liquid, 1-butyl-3-methylimidazolium tetrafluoroborate ([bmim][BF_4]), was purchased from Chengjie Chemical Ltd. Corp. (Shanghai, China). Bovine Hb was obtained from Fluka (Switzerland). The concentration of Hb stock solution, prepared by dissolving Hb in 0.05 M pH 7.0 phosphate buffer solution (PBS), was 20 mg/ml. CH_3NO_2 was from Jingchun Reagent Ltd. Corp. (Shanghai, China). The stock solution of CH_3NO_2 was prepared by directly diluted with PBS (0.1 M, pH 7.0) according to the demands. CS of low molecular weight was brought from Sigma (USA). CS hydrogel was prepared by dissolving 5 mg CS in 1 ml HAc (0.1 M). Supporting electrolyte solution for experiments was 0.1 M pH 7.0 PBS. All other chemicals were of analytical reagent grade. Deionized double-distilled water was used throughout the experiments. Unless other specified, all experiments were operated at room temperature.

All the electrochemical measurements were performed on a CHI 660A electrochemical workstation. A standard three-electrode system, with a film modified glassy carbon electrode (GCE) as the working electrode, a saturated calomel electrode (SCE) as the reference electrode and a platinum foil as the auxiliary electrode, was used in the measurements. Nitrogen atmosphere was maintained during the measurements. The pH value of electrolyte was determined by using a 320-S acidity meter (Mettler-Toledo, Switzerland). A JEOL JSM-5510LV scanning electron microscopy (SEM, Japan) was applied for characterizing the prepared samples.

2.2. Preparation of the GR-CS/Hb/GR/IL/GCE

5 μl of 1% IL-ethanol solution was first dropped onto the surface of the pretreated GCE to form the IL/GCE. Then, 5 μl of the homogeneous GR-DMF solution (1 mg/ml) was covered the IL/GCE. After drying, 10 μl Hb solutions (20 mg/ml) were spread onto the GR/IL/GCE surface. Finally, 5 μl of the resulting CS-dispersed GR solution, in which the concentration of GR was 1 mg/ml, was coated on the surface of Hb/GR/IL/GCE. The electrode referred in the text as GR-CS/Hb/GR/IL/GCE was fabricated (see supporting information, Scheme 1). For comparison, GR-CS/Hb/GR/GCE, GR-CS/Hb/IL/GCE, GR-CS/GR/IL/GCE and CS/Hb/GR/IL/GCE were also prepared by this simple drop-casting technique.

3. Results and discussion

3.1. Morphology characterization of the fabricated biosensor

The surface morphologies of GR-CS/Hb/GR/IL membrane and three different membranes were examined by SEM observation. The top views of GR (Fig. 1a) clearly illustrated the typically flake-like with slightly scrolled edges shapes, which was consistent with the previous reports (Shan et al., 2009; Xu et al., 2010a). Fig. 1b presented the SEM image of Hb film. The bright globular structures were assignable to the deposition of Hb molecules with large aggregations. As can be seen from Fig. 1c, the GR-CS/Hb/GR membrane looked rough and incompact. However, for GR-CS/Hb/GR/IL membrane (Fig. 1d), a totally different morphology was obtained. It seemed that the GR-CS/Hb/GR/IL film was characterized with uniform and smooth surface. The degree of evenness was better when IL was added, which could be attributed to the binding and blanketing effect of viscous IL (Xiao et al., 2008).

3.2. Cyclic voltammetry characterization of the biosensor

To discern the role of each component and possible synergy between them, cyclic voltammograms (CVs) of different electrodes were recorded in Fig. 2. No voltammetric response was observed for GR-CS/GR/IL/GCE except for a large background current (Fig. 2a). Whereas a pair of well-defined and nearly reversible peaks with the formal potential of −0.240 V appeared on GR-CS/Hb/GR/IL/GCE (Fig. 2b), indicating that the couple of peaks arises from the redox reaction of Hb–Fe(III)/Fe(II) (Wang et al., 2005). In comparison, the current responses of GR-CS/Hb/GR matrix without IL were faint and feeble (Fig. 2c), meaning that IL played an important role in facilitating the direct electron transfer of Hb. Although the peak currents decreased apparently and the peak-to-peak separation (ΔE_p) increased synchronously at both GR-CS/Hb/IL/GCE (Fig. 2d) and CS/Hb/GR/IL/GCE (Fig. 2e), the peak current of Hb decreased more sharply at GR-CS/Hb/IL/GCE. The phenomenon demonstrated that GR, especially close to the surface of electrode, greatly promoted the electron transfer between redox enzyme and the underlying electrode (Xu et al., 2010a). Thus, the combination of IL and GR showed an extraordinary synergisitic enhancement for the electron transfer rate of Hb enzyme.

3.3. Selection of the optimum experimental conditions

3.3.1. Influence of pH on electrochemical behaviors of the biosensor

The pH effect of supporting electrolyte on the electrochemical behaviors of Hb was explored over the range of 4.0–9.0 (see supporting information, Fig. S1). Both the anodic (E_{pa}) and cathodic (E_{pc}) potential shifted negatively with the increase of pH, implying that the electrochemical process involved proton transfer. In addition, the E_{pa}, E_{pc} and $E^{0'}$ (formal potential) were linearly dependent on the pH value of PBS with the slope values of 45, 42 and 44 mV/pH, respectively. All those slope values were smaller than the theoretical value of 57.6 mV/pH at 18 °C for a single-proton coupled

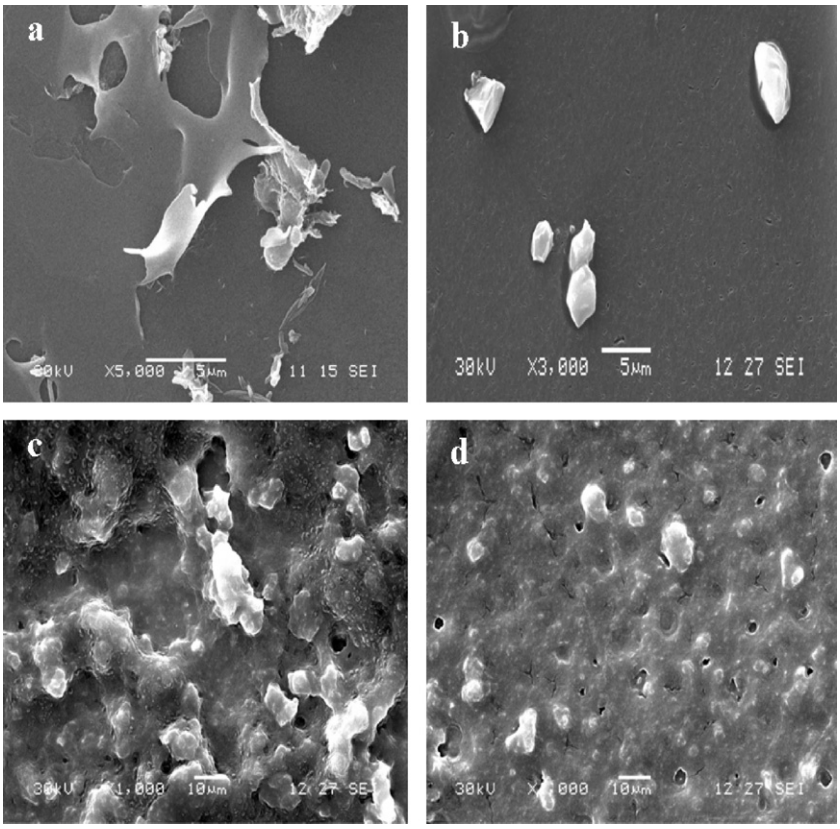

Fig. 1. SEM images of (a) GR, (b) Hb, (c) GR-CS/Hb/GR and (d) GR-CS/Hb/GR/IL on the glassy carbon.

reversible one-electron transfer (Bond, 1980; Meites, 1965). The reason for this difference might result from the influence of the protonation of trans and residue ligands around heme, or the protonation of the water molecule coordinated to the central iron (Lu et al., 2007). The anodic peak currents changed significantly in the pH range. The maximum value of peak currents was achieved at pH 7.0. So pH 7.0 was deemed as the optimum pH and used in the further experiments.

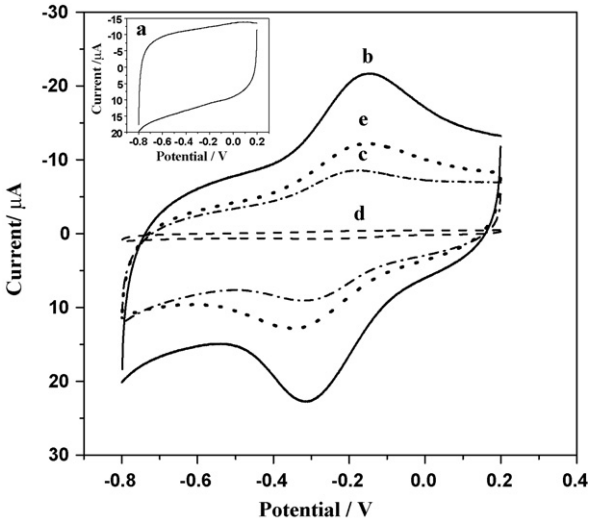

Fig. 2. CVs of (a) GR-CS/GR/IL/GCE, (b) GR-CS/Hb/GR/IL/GCE, (c) GR-CS/Hb/GR/GCE, (d) GR-CS/Hb/IL/GCE and (e) CS/Hb/GR/IL/GCE in 0.1 M pH 7.0 PBS at a scan rate of 0.1 V/s.

3.3.2. Influence of scan rate on electrochemical behaviors of the biosensor

With the increase of scan rate from 10 to 500 mV/s, the anodic and cathodic peak currents of Hb grew linearly, demonstrating that the redox process of Hb was surface-confined (Zhang et al., 2007) (see supporting information, Fig. S2). What's more, the charge consumed (Q), obtained by the integration of reduction peaks, keep almost unchanged regardless of the scan rate. According to Faraday's law, $Q = nFA\Gamma^*$ (where n is the number of electron transferred, F and A stand for the Faraday constant and the geometric area of the modified electrode surface, respectively). Therefore, the surface concentrations of electroactive Hb at GR-CS/Hb/GR/IL/GCE was estimated to be 7.70×10^{-10} mol cm^{-2}, which was about 41 times as large as the theoretical monolayer coverage (1.89×10^{-11} mol cm^{-2}) (Liu et al., 2004) and 1.8 times higher than that (4.25×10^{-10} mol cm^{-2}) at Hb/RTIL/PDDA-G/GCE (Liu et al., 2010). This revealed that multilayers of Hb participated in the electron-transfer process. The percentage of electroactivity Hb on the electrode surface was 2.19%, illuminating that only the protein molecules close to the electrode surface and with suitable orientation could exchange electrons with the electrode surface (Wang et al., 2005).

On the other hand, the peak potentials shift slightly with increasing scan rate from 0.01 to 1 V/s. However, the values of E_{pc} and E_{pa} were proportional to the logarithm of scan rates with slopes of $2.3RT/(1-\alpha)nF$ and $2.3RT/\alpha nF$ at high scan rates. So the electron transfer coefficient (α) was calculated to be 0.42. Based on the Laviron theory (Laviron, 1979), the heterogeneous electron transfer rate constant (k_s) of Hb could be determined and estimated to be 57.3 s^{-1}, which was superior to that incorporated in DDAB-HIMIMPF$_6$ (11.6 s^{-1}) (Xu et al., 2010b), SA-MWCNTs (9.54 ± 0.883 s^{-1}) (Zhao et al., 2009), and PVA/MWCNTs/CILE (1.05 s^{-1}) (Sun et al., 2009). The promotion to electron transfer of

Hb may be due to the synergetic function of GR and IL with good biocompatibility and high conductivity.

3.3.3. Influence of temperature on the detection of CH_3NO_2 by the biosensor

Under the optimal conditions established above, the effect of temperature on the current response of the biosensor to 2.12 mM CH_3NO_2 was investigated at the range from 10 to 60 °C (data not shown). It can be noted that the current increased with the temperature up to 30 °C, and then gradually decreased as the temperature further increases. The results may be attributed to the partial denaturation of Hb at high temperatures. Considering both the lifetime and current response of the biosensor, the room temperature (25 °C) was chosen as the optimum temperature in detection of CH_3NO_2.

3.4. Amperometric response of the CH_3NO_2 biosensor

As shown in Fig. 3A, there was no electrochemical response at GR-CS/GR/IL/GCE in the absence of CH_3NO_2 (curve a). However, a cathodic peak corresponding to the reductive of CH_3NO_2 was obtained at −1.01 V when CH_3NO_2 existed (curve b). In addition, it was necessary to mention that a new peak, appeared at −0.790 V with considerably higher current response, was clearly observed on the GR-CS/Hb/GR/IL/GCE when CH_3NO_2 was added into the detection solution (curve d). The presence of Hb led to the great augment in the current response of CH_3NO_2 and the rapid decline of the overpotential, which were all characteristic of electrocatalytic reduction of CH_3NO_2 by Hb. Furthermore, the decrease of the overpotential was favorable to avoid possible interferences from the electroactive substances in biological matrixes (Du et al., 2009).

There was no doubt that the current response of electrochemical biosensors was strongly dependent on the applied potentials. On the other hand, the selectivity of electrochemical biosensors is also potential-dependant. To the best of our knowledge, the coexisting biological compound, such as O_2 and NO_2^-, may interfere with the electrochemical determination of CH_3NO_2 at the more negatively potentials (Zhu et al., 2009; Wei et al., 2009). Therefore, amperometric responses of the biosensor to CH_3NO_2 were examined at different potentials ranging from −0.6 to 0 V. Among these potentials, the optimized working potential of −0.35 V was selected to ensure a relatively high sensitivity, sufficient current response, as well as relatively low background current of the biosensor. In order to demonstrate the performance of the proposed CH_3NO_2 biosensor, a comparison of the amperometric response of the GR-CS/Hb/GR/IL/GCE with that of the other modified electrodes at the applied potential of −0.35 V was displayed in Fig. 3B. For both the GR-CS/GR/IL/GCE (curve b) and CS/Hb/IL/GCE (curve c), the vision of small current response was caught. In contrast, the largest stepped growth of reduction current could be seen at GR-CS/Hb/GR/IL/GCE (curve a). It was inferred that the synergistic effect of the electrocatalytic activity of Hb and GR resulted in the better catalytic property of GR-CS/Hb/GR/IL/GCE toward CH_3NO_2 than that of other cases. It was known from the inset of Fig. 3B that the GR-CS/Hb/GR/IL/GCE had an excellent linear response to CH_3NO_2 in the concentration range from 2.0×10^{-9} to 2.3×10^{-7} M with a correlation coefficient of 0.9991, which was much wider than that of 2.0×10^{-9}–7.5×10^{-8} M at CS/Hb/IL/GCE. A low detection limit of 6.0×10^{-10} M ($S/N = 3$) was obtained by the prepared biosensor, which was evidently lower than the value of 3.3×10^{-5} M by Mb/ddab/PG electrode (Jean and Mekki, 2004) and was also comparable to that of 1.6×10^{-10} M by SPME-GC–HRMS method (Alwis et al., 2008). The sensitivity of the biosensor (788 μA mM^{-1}) was improved apparently compared with that of 329 μA mM^{-1} at GR-CS/GR/IL/GCE and 211 μA mM^{-1} at CS/Hb/IL/GCE. Moreover, 95% of the steady-state current was

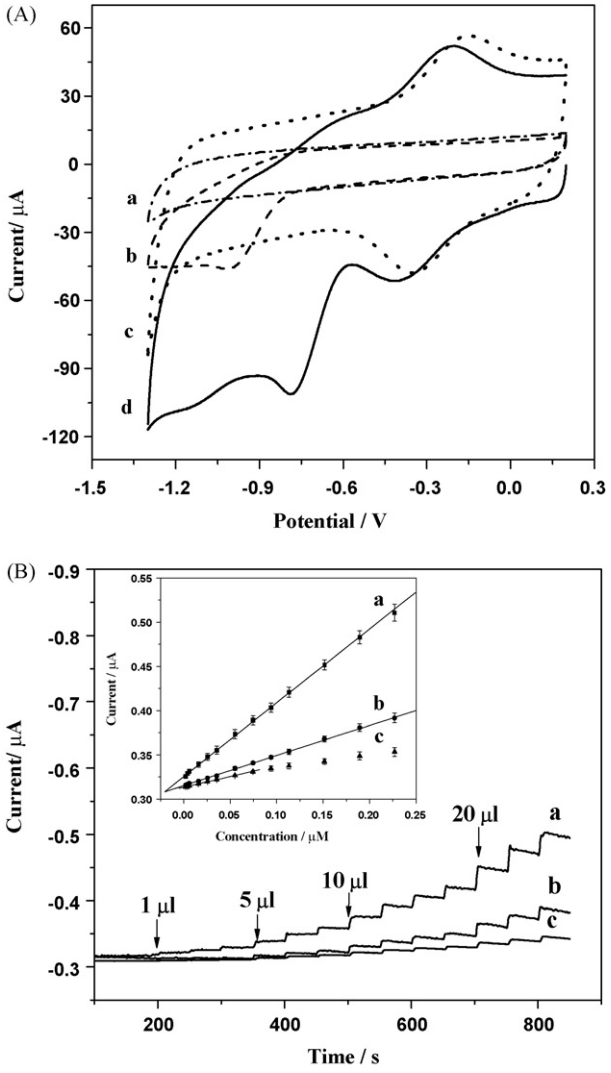

Fig. 3. (A) CVs at 0.1 V/s in 0.1 M pH 7.0 PBS for (a) GR-CS/GR/IL/GCE and (c) GR-CS/Hb/GR/IL/GCE without CH_3NO_2; (b) GR-CS/GR/IL/GCE and (d) GR-CS/Hb/GR/IL/GCE in buffer containing 2.12 mM CH_3NO_2. (B) Amperometric response of (a) GR-CS/Hb/GR/IL/GCE, (b) GR-CS/GR/IL/GCE and (c) CS/Hb/IL/GCE upon successive additions of 7.92 μM CH_3NO_2 into stirring 0.1 M pH 7.0 PBS. Applied potential: −0.35 V. Inset: the corrected curves of catalytic current (I_{cat}) against CH_3NO_2 concentration for (a) GR-CS/Hb/GR/IL/GCE, (b) GR-CS/GR/IL/GCE and (c) CS/Hb/IL/GCE in 0.1 M pH 7.0 PBS. The relative standard deviation (RSD) is less than 7%.

reached within 5 s when aliquots of CH_3NO_2 were added, indicating the rapid response of the biosensor. Such fast response may be on account of the introduction of GR and the easy diffusion of substrate in the GR-CS/Hb/GR/IL matrix. The calibration curve tended to level off when the concentration of CH_3NO_2 became larger, manifesting the characteristics of the Michaelis–Menten kinetic mechanism. The apparent Michaelis–Menten constant (K_m^{app}) for the biosensor to CH_3NO_2 was calculated to be 0.16 μM according to the Lineweaver–Burk equation (Kamin and Wilson, 1980), which was remarkably lower than the value reported by Mb/ddab/PG electrode (Jean and Mekki, 2004). The low K_m^{app} value suggested that Hb in GR-CS/Hb/GR/IL membrane retained its bioelectrocatalytic activity and exhibited a high affinity to CH_3NO_2.

3.5. Reproducibility and stability of the biosensor

The relative standard deviation (RSD) was 5.41% for 10 successive determinations of 1.36×10^{-7} M CH_3NO_2 using one single GR-CS/Hb/GR/IL/GCE. The result illuminated that the biosensor

showed the excellent reproducibility for the determination of CH_3NO_2. The stability of the biosensor was also investigated. The biosensor could maintain 90% of its initial response after being stored for 50 days in the refrigerator. As expected, the biosensor posed outstanding long-time storage stability, which might be due to the following aspects. Firstly, the unique sandwich-like structures of GR-CS/Hb/GR/IL matrix could provide a favorable microenvironment for Hb to remain its conformation and bioactivity. Additionally, the out layer of GR-CS hybrid film could efficiently prevent the leakage of the bound Hb (Xu et al., 2010a; Zhang et al., 2007). Owing to the above advantages, it can be seen that this method was reliable for the determination of CH_3NO_2.

3.6. Selectivity and application of the biosensor

The influence of the interfering species on 7.84×10^{-8} M CH_3NO_2 determination was examined. It was found that 1000-fold NO_3^-, C_7H_8, $C_6H_5NO_2$ did not interfere with the test of CH_3NO_2. The good selectivity of the biosensor might be related to the low working potential of −0.35 V. To demonstrate the application potential of the biosensor in environmental analysis, real freshwater samples detection was performed. It was found that the CH_3NO_2 content in the tested samples was too low to be detected by the biosensor (data not shown). However, there is an evident increase in the current response if different concentrations of CH_3NO_2 were added into the samples. This suggested that the proposed biosensor could be applied to the determination of CH_3NO_2 in environment samples, with a linear range from 9.9×10^{-9} to 4.0×10^{-7} M and a sensitivity of 353 $\mu A\,mM^{-1}$. Although the results of CH_3NO_2 analysis were not so satisfied in real samples, it is still an area that we will be working hard to improve.

4. Conclusion

In this paper, the employment of GR nanosheets, IL and biopolymer (CS) associated with the inherent catalytic activity of Hb toward CH_3NO_2, provide us to fabricate a new CH_3NO_2 biosensor. This biosensor offered several fascinating advantages: first, the especial sandwich structure of the biosensor could provide a friendly microenvironment for Hb to preserve its native structure and bioactivity. Second, the appearance of GR and IL with high conductivity and prominent biocompatibility greatly promoted the direct electron transfer between Hb and the underlying electrode. Therefore, the biosensor achieved a limit of detection down to 6.0×10^{-10} M for quantitative CH_3NO_2 analysis. In addition, the constructed biosensor displayed high sensitivity, enhanced affinity, and a prolonged good stabilization to the detection of CH_3NO_2. Although the determination of CH_3NO_2 in real samples by the biosensor is in the improvement stages, we still believe this approach can pave a new and cost-effective way for biomonitoring of CH_3NO_2 both in methodological study and in clinical laboratories.

Acknowledgements

This work was supported by the National Natural Science Foundation of China (No. 20875023).

Appendix A. Supplementary data

Supplementary data associated with this article can be found, in the online version, at doi:10.1016/j.bios.2010.08.027.

References

Alwis, K.U., Blount, B.C., Smith, M.M., Loose, K.H., 2008. Environ. Sci. Technol. 42, 2522–2527.
Bond, A.M., 1980. Modern Polarographic Methods in Analytical Chemistry. Marcel Dekker, New York.
Chen, H.J., Wang, Y.L., Liu, Y., Wang, Y.Z., Qi, L., Dong, S.J., 2007. Electrochem. Commun. 9, 469–474.
Chen, F., Qing, Q., Xia, J.L., Li, J.H., Tao, N.J., 2009. J. Am. Chem. Soc. 131, 9908–9909.
Du, D., Wang, J., Smith, J.N., Timchalk, C., Lin, Y.H., 2009. Anal. Chem. 81, 9314–9320.
Fainberg, A., 1992. Science 255, 1531–1537.
Jean, B., Mekki, B., 2004. Inorg. Chem. 43, 3847–3853.
Jones, L.R., Riddick, J.A., 1956. Anal. Chem. 28, 1493–1495.
Kamin, R.A., Wilson, G.S., 1980. Anal. Chem. 52, 1198–1205.
Kang, X.H., Wang, J., Wu, H., Aksay, I.A., Liu, J., Lin, Y.H., 2009. Biosens. Bioelectron. 25, 901–905.
Laviron, E., 1979. J. Electroanal. Chem. 101, 19–28.
Liu, H.H., Tian, Z.Q., Lu, Z.X., Zhang, Z.L., Zhang, M., Pang, D.W., 2004. Biosens. Bioelectron. 20, 294–304.
Liu, Q., Hu, C.G., Cui, R., Hu, S.S., 2007. J. Phys. Chem. B 111, 9808–9813.
Liu, K.P., Zhang, J.J., Yang, G.H., Wang, C.M., Zhu, J.J., 2010. Electrochem. Commun. 12, 402–405.
Lu, Q., Hu, C.G., Cui, R., Hu, S.S., 2007. J. Phys. Chem. B 111, 9808–9813.
Meaney, M.S., McGuffin, V.L., 2008. Anal. Chim. Acta 610, 57–67.
Meites, L., 1965. Polarographic Techniques, second ed. Wiley, New York.
Moulthrop, J.S., Swatloski, R.P., Moyna, G., Rogers, R.D., 2005. Chem. Commun. 12, 1557–1559.
Page, E.H., Pajeau, A.K., Arnold, T.C., Fincher, A.R., Goddard, M.J., 2001. Am. J. Ind. Med. 40, 107–113.
Quinn, B.M., Ding, Z.F., Moulton, R., Bard, A.J., 2002. Langmuir 18, 1734–1742.
Sabourin, J.L., Dabbs, D.M., Yetter, R.A., Dryer, F.L., Aksay, I.A., 2009. ACS Nano 3, 3945–3954.
Shan, C.S., Yang, H.F., Song, J.F., Han, D.X., Ivaska, A., Niu, L., 2009. Anal. Chem. 81, 2378–2382.
Shan, C.S., Yang, H.F., Han, D.X., Zhang, Q.X., Ivaska, A., Niu, L., 2010. Biosens. Bioelectron. 25, 1504–1508.
Singh, S., 2007. J. Hazard. Mater. 144, 15–28.
Stankovich, S., Dikin, D.A., Dommett, G.H.B., Kohlhaas, K.M., Zimney, E.J., Stach, E.A., Piner, R.D., Nguyen, S.T., Ruoff, R.S., 2006. Nature 442, 282–286.
Subirats, X., Porras, S.P., Roses, M., Kenndler, E., 2005. J. Chromatogr. A 1079, 246–253.
Sun, W., Li, X.Q., Wang, Y., Zhao, R.J., Jiao, K., 2009. Electrochim. Acta 54, 4141–4148.
Tang, J., Wang, B., Wu, Z., Han, X., Dong, S., Wang, E., 2003. Biosens. Bioelectron. 18, 867–872.
Wang, J., Bansenauer, B.A., Koel, B.E., 1998. Langmuir 14, 3255–3263.
Wang, S.F., Chen, T., Zhang, Z.L., Shen, X.C., Lu, Z.X., Pang, D.W., Wong, K.Y., 2005. Langmuir 21, 9260–9266.
Wang, Y., Li, Y.M., Tang, L.H., Lu, J., Li, J.H., 2009. Electrochem. Commun. 11, 889–892.
Wei, W., Jin, H.H., Zhao, G.C., 2009. Microchim. Acta 164, 167–171.
Xiao, F., Liu, L.Q., Li, J., Zeng, J.J., Zeng, B.Z., 2008. Electroanalysis 18, 2047–2054.
Xu, H., Xiong, H.Y., Zeng, Q.X., Jia, L., Wang, Y., Wang, S.F., 2009. Electrochem. Commun. 11, 286–289.
Xu, H.F., Dai, H., Chen, G.N., 2010a. Talanta 81, 334–338.
Xu, Y.X., Hu, C.G., Hu, S.S., 2010b. Anal. Chim. Acta 663, 19–26.
Zhang, M., Smith, A., Gorski, W., 2004. Anal. Chem. 76, 5045–5050.
Zhang, Q., Zhang, L., Li, J.H., 2007. J. Phys. Chem. C 111, 8655–8660.
Zhao, H.Y., Zheng, W., Meng, Z.X., Zhou, H.M., Xu, X.X., Li, Z., Zheng, Y.F., 2009. Biosens. Bioelectron. 24, 2352–2357.
Zhu, A.W., Tian, Y., Liu, H.Q., Luo, Y.P., 2009. Biomaterials 30, 3183–3188.